Am J Cancer Res 2023;13(11):5443-5454
www.ajcr.us /ISSN:2156-6976/ajcr0152643

*Original Article*

# Characteristics of the immune microenvironment associated with RRM2 expression and its application to PD-L1/PD-1 inhibitors in lung adenocarcinoma

Seul-Ki Lee[1], Yoonjung Hwang[1], Jae-Ho Han[1], Seokjin Haam[2], Hyun Woo Lee[3], Young Wha Koh[1]

*[1]Department of Pathology, Ajou University School of Medicine, Suwon-si, Gyeonggi-do, South Korea; [2]Department of Thoracic and Cardiovascular Surgery, Ajou University School of Medicine, Suwon-si, Gyeonggi-do, South Korea; [3]Department of Hematology-Oncology, Ajou University School of Medicine, Suwon-si, Gyeonggi-do, South Korea*

Received August 6, 2023; Accepted November 6, 2023; Epub November 15, 2023; Published November 30, 2023

**Abstract:** Recent studies have indicated that RRM2 plays a crucial part in the tumor immune microenvironment. According to the expression of RRM2, we evaluated immune cell infiltration, immunotherapy biomarkers, and the expression of immune checkpoint molecules in four lung adenocarcinoma (LUAD) datasets. We employed the Tumor Immune Dysfunction and Exclusion (TIDE) and CIBERSORTx algorithms to examine the patterns of immune cell distribution and evaluate the responses to anti-programmed death protein-1/programmed death ligand-1 (PD-1/PD-L1) therapy in three publicly available LUAD datasets. These findings were corroborated using a validation group comprising patients who received treatment with PD-1/PD-L1 inhibitors. Additionally, we conducted experiments using LUAD cell lines to investigate how RRM2 affects the expression of PD-L1. In comparison to the low RRM2 group, the high RRM2 group exhibited a high interferon gamma signature, high T-cell-inflamed signature, high CD274 expression, high CD8+ T cell levels, low cancer-associated fibroblasts, and low M2 macrophages, according to TIDE analysis in the three LUAD datasets. Analysis of the three LUAD datasets using CIBERSORTx confirmed a positive correlation between RRM2 and CD8+ T cells, and this finding was validated by immunohistochemistry in a separate validation set. In the three LUAD datasets without PD-1/PD-L1 inhibitor treatment, higher RRM2 expression was associated with a poorer prognosis. However, in the LUAD dataset treated with PD-1/PD-L1 inhibitors, higher RRM2 expression was associated with better prognosis. In the three datasets, the high-RRM2 group exhibited higher expression of inhibitory immune checkpoint molecules. In a LUAD cell line study, we discovered that RRM2 regulates PD-L1 expression through the ANXA1/AKT pathway. The expression of RRM2 shows promise as a predictive biomarker for PD-1/PD-L1 inhibitors in LUAD patients, and it may represent a new target to overcome resistance to PD-L1/PD-1 therapies.

**Keywords:** Lung adenocarcinoma, RRM2, PD-L1, PD-1, CD8, macrophage

## Introduction

Programmed death protein-1/programmed death ligand-1 (PD-1/PD-L1) inhibitor blockade is an effective therapeutic approach to improve prognosis for advanced non-small cell lung cancer (NSCLC) [1-3]. While PD-L1 protein expression levels have been used to predict clinical responses to PD-L1/PD-1 inhibitors, NSCLC patients with minimal or absent PD-L1 expression have also demonstrated long-lasting responses [4, 5]. Our current understanding of the mechanisms underlying tumor immune resistance remains incomplete, emphasizing the need for improved predictive biomarkers of PD-L1/PD-1 blockades.

Ribonucleotide reductase (RR) is an essential enzyme that facilitates deoxyribonucleotide synthesis during DNA replication [6]. RR primarily comprises two homodimeric subunits: a large subunit (RRM1) and a small subunit (RRM2) [6]. Alterations in RRM2 can potentially result in genome instability and increased mutation rates, thereby affecting tumor advancement [7, 8]. Elevated RRM2 levels have been documented in various cancer types [9] and are associated with tumor progression and

**Table 1.** Demographic and clinical characteristics of patients

| | Pancancer Atlas (n = 510) | Oncosg (n = 169) | Cptac (n = 110) | Validation (n = 343) |
|---|---|---|---|---|
| Age, median (range) | 66 (38-88) | 64 (37-84) | 62 (35-81) | 63 (31-86) |
| Male sex | 236 (46.3%) | 75 (44.4%) | 72 (65.5%) | 211 (61.5%) |
| TNM | | | | |
| Stage I | 277 (54.3%) | 102 (60.4%) | 46 (41.8%) | 153 (45.5%) |
| Stage II | 123 (24.1%) | 30 (17.8%) | 17 (15.5%) | 39 (11.6%) |
| Stage III | 83 (16.3%) | 31 (18.3%) | 13 (11.8%) | 92 (27.4%) |
| Stage IV | 27 (5.3%) | 4 (2.4%) | 0 (0%) | 52 (15.5%) |
| EGFR Mutant | 66 (12.9%) | 93 (55%) | 38 (34.5%) | 83 (48.8%) |
| ALK rearrangement | 5 (1%) | 6 (3.6%) | 0 (0%) | 3 (2%) |
| Smoking history presence | N/A | 61 (36.1%) | 56 (54.9%) | 161 (56.7%) |
| PD-1/PD-L1 inhibitor treatment | None | None | None | 63 (18.4%) |

N/A: not applicable. In the validation set, records of TNM stage, EGFR mutation, ALK rearrangement, and smoking history were available for 336, 170, 147, and 284 individuals, respectively.

metastasis [10, 11]. Recent studies have shown that RRM2 plays a significant role in the immune microenvironment. It has been found to have a positive regulatory effect on PD-L1 expression in renal cell carcinoma (RCC) [12]. It also influences the immune response in RCC by modulating the ANXA1/AKT signaling axis [12]. The expression of RRM2 was significantly positively correlated with immune cell infiltration, immune cell biomarkers, and immune checkpoint expression in hepatocellular carcinoma (HCC) [11]. In vitro and in vivo studies have revealed that RRM2 inhibition effectively induces M1 macrophage polarization while suppressing M2 macrophage polarization in lung adenocarcinoma (LUAD) [13]. Our previous study revealed that an intrinsic pathway-associated gene signature, including RRM2, was associated with improved prognosis in patients who received PD-L1/PD-1 inhibitor therapy in LUAD [14].

However, studies investigating the impact of RRM2 on the tumor immune microenvironment in the field of lung cancer are rare. We evaluated immune cell infiltration, immune cell biomarkers, and immune checkpoint expression in three public LUAD databases according to RRM2 expression using the Tumor Immune Dysfunction and Exclusion (TIDE) and CIBERSORTx tools. The results that were consistently identified across the three LUAD public databases were further confirmed in the LUAD validation set using immunohistochemical staining. Finally, we examined whether RRM2 mRNA or protein expression could serve as a predictive biomarker in patients receiving PD-L1/PD-1 inhibitor therapy.

## Materials and methods

### *Study population*

Four LUAD datasets were examined, including three public gene expression datasets consisting of 510, 169, and 110 samples and one validated dataset with 343 samples. Three LUAD-related mRNA datasets were obtained from the cBioportal database (http://cbioportal.org) [15]. **Table 1** summarizes the demographic and clinical features of the four datasets. RRM2 mRNA data from LUAD patients who received PD-L1/PD-1 inhibitor therapy were obtained from a previous study [14]. The Institutional Review Board of Ajou University School of Medicine approved this study (AJOUIRB-KSP-2020-396 and 2020-12-28). Informed consent was waived due to the retrospective study design.

### *TIDE and CIBERSORTx tool*

Nine predictive biomarkers for PD-L1/PD-1 inhibition were identified using the TIDE tool: TIDE, interferon gamma gene signature, microsatellite instability (MSI), T-cell-inflamed signature, CD274 (PD-L1), CD8, myeloid-derived suppressor cells (MDSC), cancer-associated fibroblasts (CAF) and Tumor-associated macrophage M2 (TAM_M2) [16]. The CIBERSORTx

tool was used to identify the CD8 and TAM-M2 levels in LUAD samples [17].

*Immunohistochemistry of PD-L1, RRM2 and CD8*

A tissue microarray was used to conduct immunochemical staining on the surgically resected samples. Biopsy samples were obtained from all sections for analysis. Anti-RRM2 (clone 1E1; Abcam) and anti-CD8 (clone C8/144B, DAKO) antibodies were used for analyses. A VENTANA BenchMark ULTRA instrument was used to perform the PD-L1 SP263 assay using the OptiView DAB Immunohistochemical Detection Kit [18]. RRM2 or PD-L1 staining levels were categorized into four groups (0, 1, 2, and 3) to determine their intensity. Additionally, the percentage of cytoplasmic or membrane expression was assessed. H-scores were used to analyze the staining intensities of RRM2 and PD-L1 [19]. In order to assess CD8 immunostaining, the number of membrane-positive cells was measured at three different locations, and the average value was subsequently calculated.

*Cell lines and transfection*

The Korean Cell Line Bank provided the A549, NCI-H441, and NCI-H650 human LUAD cell lines. A549 cells were grown using DMEM, while NCI-H441 and NCI-H650 cells were cultured using RPMI 1640 medium. The cells were incubated in RPMI 1640 medium at a temperature of 37°C in a humid environment with 5% $CO_2$. The culture medium contained 10% fetal bovine serum and 1% penicillin-streptomycin as supplements. Prior to experimentation, all the cell lines were tested to ensure that there was no mycoplasma contamination. The siRNA was introduced into the cells through transfection using Lipofectamine RNAiMAX Reagent (Invitrogen), in accordance with the guidelines provided by the manufacturer.

The specific siRNA sequences used to target RRM2 were as follows: siRNA #1 (5'-CACAAGGCGAUAAUAGCUU-3' and 5'-AAGCUAUUAUCGCCUUGUG-3') and siRNA #2 (5'-GAGCUAAGGUAGUAUUGUA-3' and 5'-UACAAUACUACCUUAGCUC-3').

*Western blotting*

The cells were subjected to lysis using RIPA lysis buffer (Thermo Fisher Scientific Inc.), followed by separation through sodium dodecyl sulfate-polyacrylamide gel electrophoresis. Subsequently, they were transferred onto nitrocellulose membranes and probed with specific antibodies. Antibodies against RRM2 (clone 1E1; Abcam), PD-L1 (clone 2B11D11; Proteintech), AKT (polyclonal; Proteintech), and ANXA1 (clone D5V2T; Cell Signaling Technology) were used. Protein levels were visualized using an Odyssey Infrared Imaging System (LI-COR Biosciences). The process was replicated on three separate occasions to ensure consistent results.

*Statistical analyses*

We employed the Mann Whitney U test to examine the difference between two sets of continuous variables. We used Spearman's rank correlation coefficient to calculate the correlation between two groups. We applied receiver operating characteristic (ROC) curve analysis to determine the cutoff for RRM2. We conducted survival analyses by employing both the Kaplan-Meier estimator and the Cox proportional hazard model. The statistical software programs IBM SPSS Statistics for Windows (version 25.0; IGM Inc., Armonk, NY, USA) and R version 3.5.3 (http://www.r-project.org/) were utilized for all data analyses. Statistical significance was determined by considering $p$ values less than 0.05.

## Results

*Association between RRM2 expression and predictive biomarkers for anti-PD-1/PD-L1 therapy*

We investigated the differences in the predicted biomarkers of anti-PD-1/PD-L1 therapy based on RRM2 expression in three publicly available LUAD datasets (**Figure 1**). The cutoff value of RRM2 mRNA was 890 in the PanCancer Atlas, -0.04 in the OncoSG dataset, and 3.09 in the CPTAC dataset. We included only parameters with $p$-values less than 0.1 from all three groups shown in **Figure 1**. Across the three datasets, the interferon gamma signature was significantly higher in the group with high RRM2 than in the group with low RRM2 ($P < 0.001$ for the PanCancer Atlas, $P = 0.001$ for the Oncosg dataset, and $P = 0.016$ for the CPTAC dataset). The group with high RRM2 had a greater T cell-inflamed signature than the group with low RRM2 in the three datasets (P =

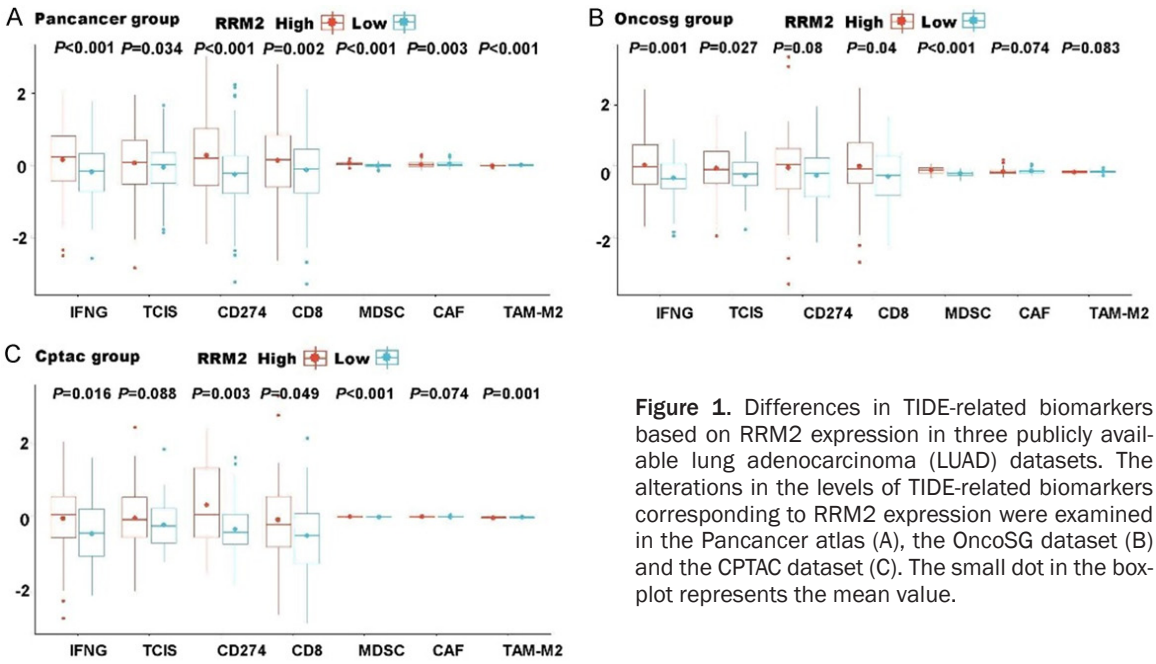


**Figure 1.** Differences in TIDE-related biomarkers based on RRM2 expression in three publicly available lung adenocarcinoma (LUAD) datasets. The alterations in the levels of TIDE-related biomarkers corresponding to RRM2 expression were examined in the Pancancer atlas (A), the OncoSG dataset (B) and the CPTAC dataset (C). The small dot in the boxplot represents the mean value.

0.034 for the PanCancer Atlas, 0.027 for the OncoSG dataset, and 0.088 for the CPTAC dataset). In the three datasets, we found that the group with high RRM2 had a greater level of CD274 expression compared to the group with low RRM2 ($P < 0.001$ for the PanCancer Atlas, $P = 0.08$ for the OncoSG dataset, and $P = 0.003$ for the CPTAC dataset). The CD8+ T cell level was significantly greater in the high RRM2 group as compared to the low RRM2 group in the three different datasets ($P = 0.002$ for the PanCancer Atlas, $P = 0.04$ for the OncoSG dataset, and $P = 0.049$ for the CPTAC dataset). The group with high RRM2 showed a significantly elevated level of MDSC compared to the group with low RRM2 in three different datasets ($P < 0.001$ for the PanCancer Atlas, $P < 0.001$ for the OncoSG dataset, and $P < 0.001$ for the CPTAC dataset). Across the three datasets, the group with high RRM2 had a reduced level of CAF compared to the group with low RRM2 ($P = 0.003$ for PanCancer Atlas, $P = 0.074$ for the OncoSG dataset, and $P = 0.074$ for the CPTAC dataset). Across the three datasets, the group with high RRM2 had a lower level of TAM-M2 compared to the group with low RRM2 ($P < 0.001$ for the PanCancer Atlas, $P = 0.083$ for the OncoSG dataset, and $P = 0.001$ for CPTAC dataset). However, TIDE and MSI scores did not yield consistent results across the three datasets.

*Relationship among RRM2, PD-L1 and CD8 expression in validation dataset*

Higher RRM2 expression was associated with an increase in PD-L1 expression and CD8+ T cell numbers, and a decrease in TAM-M2 cells in all three public datasets. We revalidated the results of CD8+ T cells and TAM-M2 from the TIDE analysis using Cibersortx, a tool for analyzing the distribution of immune cells. In the PanCancer and CPTAC datasets, there was a statistically significant increase in CD8+ T cell levels in the high-RRM2 group ($P < 0.001$ for the PanCancer Atlas, and $P = 0.003$ for the CPTAC dataset, as shown in **Figure 2A**). In the OncoSG dataset, there was a trend of higher CD8+ T cell levels in the high-RRM2 group; however, this was not statistically significant ($P = 0.101$; **Figure 2A**). However, there was no correlation between RRM2 and TAM2-M2 across the three datasets ($P = 0.527$ for the PanCancer Atlas, $P = 0.522$ for the OncoSG dataset, and $P = 0.24$ for the CPTAC dataset, as shown in **Figure 2A**). Since only the results of CD8+ T cells were found to be significant in the TIDE and CiberSortx analyses, we performed validation using immunohistochemistry on RRM2, CD8+ T cells and PD-L1 in the validation set. The cutoff value for RRM2 IHC was 55 in the validation set. In both the tumor and peritumoral regions, the high-RRM2 group exhibited ele-

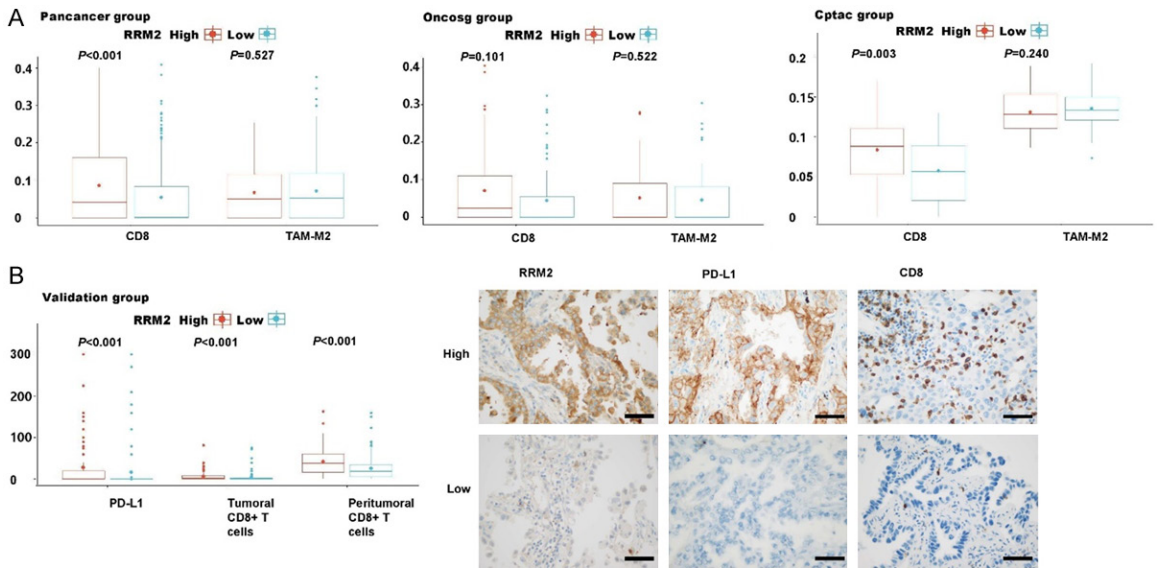


**Figure 2.** Variations in CD8 and TAM-M2 levels based on RRM2 expression in three public lung adenocarcinoma (LUAD) datasets using the CIBERSORTx tool. Changes in levels of CD8 and TAM-M2 according to RRM2 expression in the Pancancer Atlas, the OncoSG dataset and the CPTAC dataset (A). Differences in PD-L1 and CD8+ T cells were determined according to RRM2 expression in the validation dataset using immunohistochemistry. Changes in levels of PD-L1 and CD8+ T cells according to RRM2 expression (B). Representative immunohistochemical images illustrating the expression of RRM2, PD-L1, and CD8 (magnification ×400 and scale bar is 50 um) (B). The small dot in the boxplot is the mean value.

vated levels of CD8+ T cells compared to the low-RRM2 groups ($P < 0.001$ for CD8+ T cells in the tumoral region, and $P < 0.001$ for CD8+ T cells in the peritumoral region; **Figure 2B**). A positive correlation was observed between higher levels of RRM2 immunohistochemical expression and increased levels of tumoral PD-L1 ($P < 0.001$; **Figure 2B**).

*Prognostic role of RRM2 expression*

We examined how RRM2 mRNA expression could predict outcomes using publicly available datasets. We conducted survival analysis only on the PanCancer Atlas and OncoSG datasets because the CPTAC dataset did not contain survival data. The cutoff value of RRM2 mRNA was 890 in the PanCancer Atlas and -0.04 in the OncoSG dataset. In both datasets, there was a statistically significant decrease in survival rate when RRM2 mRNA expression was high ($P = 0.001$ for the PanCancer Atlas as shown in **Figure 3A**, and $P = 0.02$ for the OncoSG dataset as shown in **Figure 3B**). In the multivariate analyses, RRM2 mRNA expression was a statistically significant independent prognostic factor in the PanCancer Atlas dataset ($P = 0.012$, Supplementary Table 1); However, it was borderline significant in the OncoSG dataset ($P = 0.057$, Supplementary Table 2). Survival analysis was performed using the validation set. In the validation set, the cutoff value for RRM2 IHC was 55 in cases without PD-L1/PD-1 treatment. In the validation set, among patients who did not receive PD-L1/PD-1 therapy, high RRM2 expression was associated with a significantly worse prognosis ($P < 0.001$, **Figure 3C**). Multivariate analyses revealed that RRM2 expression was a significant independent prognostic factor in patients who did not received PD-L1/PD-1 therapy, with a statistically significant $p$ value of < 0.001 (Supplementary Table 3). In the validation set, the cut-off for RRM2 mRNA was 2168, and the cut-off for RRM2 IHC was 90 in cases with PD-L1/PD-1 treatment. However, in the validation set, there was a statistically significant improvement in the prognosis associated with high RRM2 mRNA or immunohistochemical expression among patients who received PD-L1/PD-1 therapy ($P = 0.02$, mRNA dataset, **Figure 3D**; $P = 0.027$, immunohistochemical dataset, **Figure 3E**). In patients who received PD-L1/PD-1 therapy, multivariate analyses showed that RRM2 expression was an independent prognostic factor in the mRNA dataset with a statistically significant $p$ value of 0.021 (Supplementary Table 4). However, it was

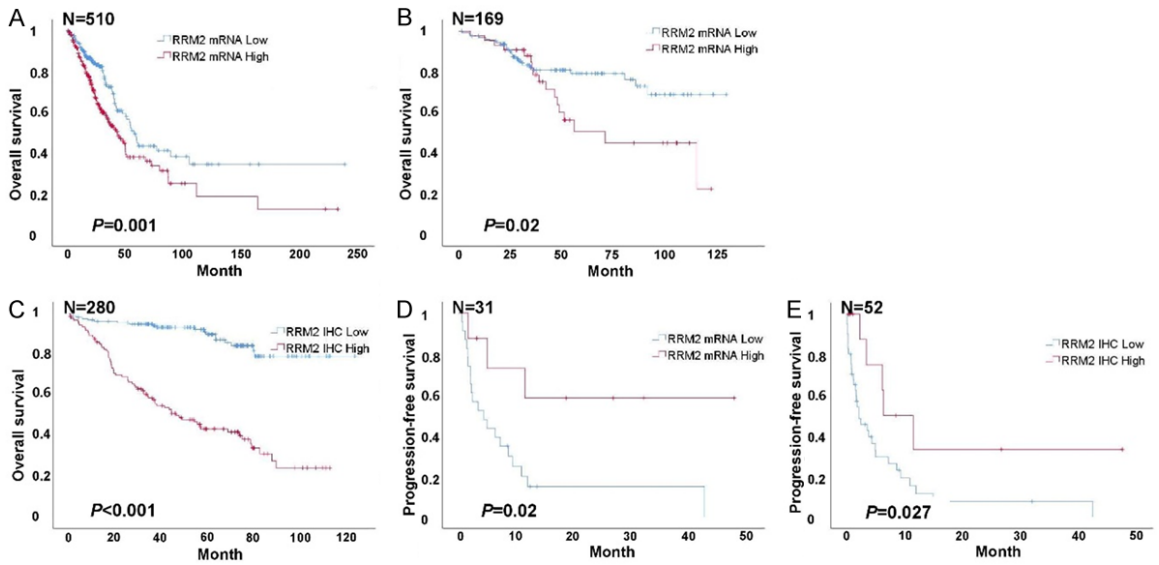


**Figure 3.** Survival analyses according to RRM2 expression. A. Overall survival (OS) according to RRM2 expression in the PanCancer cohort without PD-L1/PD-1 treatment. B. OS according to RRM2 expression in the OncoSG cohort without PD-L1/PD-1 treatment. C. OS according to RRM2 expression in validation immunohistochemical cohort without PD-L1/PD-1 treatment. D. Progression-free survival (PFS) according to RRM2 expression in validation mRNA cohort with PD-L1/PD-1 treatment. E. PFS according to RRM2 expression in validation immunohistochemical cohort with PD-L1/PD-1 treatment.

| | | PD-1 | PD-L2 | CTLA4 | TIGIT | LAG3 | VISTA | TIM3 |
|---|---|---|---|---|---|---|---|---|
| Pancancer | RRM2 | 0.15 | 0.169 | X | X | 0.216 | -0.216 | X |
| Oncosg | RRM2 | 0.298 | X | 0.264 | 0.24 | 0.365 | -0.214 | X |
| Cptac | RRM2 | 0.274 | 0.194 | 0.204 | X | 0.394 | X | 0.208 |

**Figure 4.** Correlation analysis between RRM2 and other immune checkpoint targets in three public lung adenocarcinoma (LUAD) datasets.

of borderline significance in the immunohistochemical dataset with a *p* value of 0.089 (Supplementary Table 5).

*Relationship among RRM2 and immune checkpoints in three public datasets*

In three public datasets and one validation set, RRM2 expression was positively correlated with PD-L1 and CD8+ T cells. Therefore, assuming that the immune microenvironment in the high-RRM2 group was dysregulated, we analyzed the correlation between RRM2 and other immune checkpoints. In the Pancancer Atlas dataset, RRM2 expression was significantly positively correlated with PD-1, PD-L2, and LAG3 expression (**Figure 4**). In the OncoSG dataset, there was a significant positive association between RRM2 expression and immune checkpoint molecules PD-1, CTLA4, TIGIT, and LAG3 (**Figure 4**). In the CPTAC dataset, a significant positive correlation was found between RRM2 expression and the immune checkpoint markers PD-1, PD-L2, CTLA4, LAG3, and TIM3 (**Figure 4**).

*Inhibition of RRM2 downregulate of PD-L1 through ANXA1/AKT pathway*

We confirmed a positive correlation between RRM2 and PD-L1 at both the mRNA and immunohistochemical levels and therefore investigated whether the same result was observed at the cell line level. NCI-H441 cells showed the highest expression of both PD-L1 and RRM2 among the three LUAD cell lines, indicating a positive correlation between PD-L1 and RRM2 (**Figure 5A**). A previous study has indicated that the ANXA1/AKT pathway is involved in the upregulation of PD-L1 expression by RRM2 in renal cancer [12]. In our study, RRM2 knockdown also reduced the levels of PD-L1, AKT, and ANXA1 in NCI-H441 cells (**Figure 5B**).

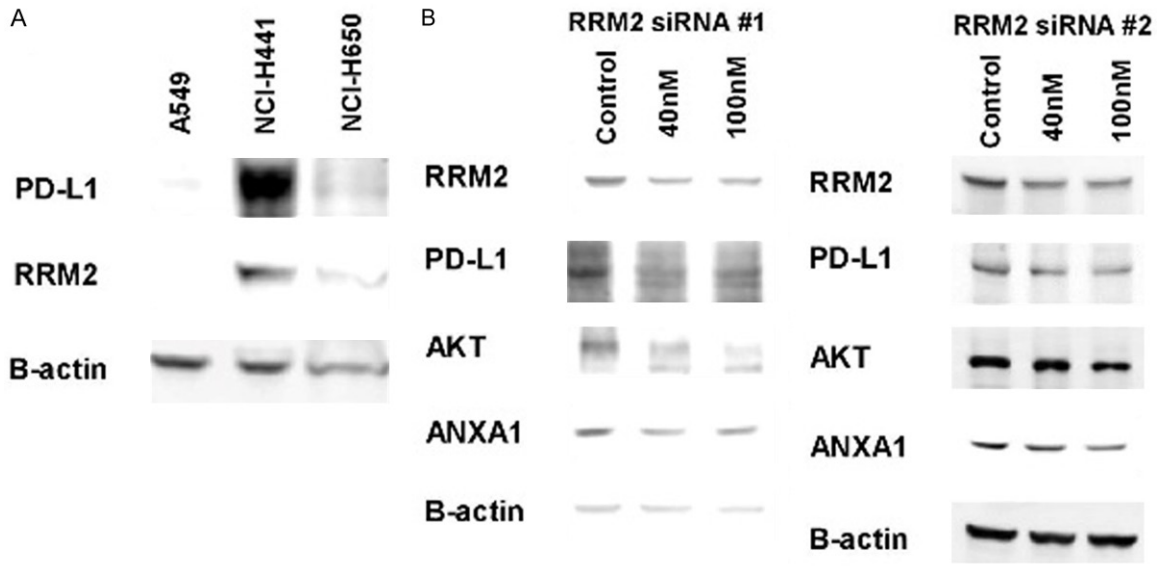


**Figure 5.** Loss of RRM2 decreases PD-L1 expression in the lung adenocarcinoma (LUAD) cell line. A. Protein levels of PD-L1 and RRM2 in various LUAD cell lines. B. Control and RRM2-knockdown in NCI-H441 cell line.

## Discussion

In the present study, a positive correlation between RRM2 expression and CD8+ T cells was observed in all four datasets. Furthermore, in experiments targeting various types of cancers, including head and neck squamous cell carcinoma, kidney renal clear cell carcinoma, and kidney renal papillary cell carcinoma, a statistically significant positive correlation between RRM2 expression and CD8+ T cells was also observed [9]. Cytotoxic CD8+ T cells, which play a crucial role in the immune response against cancer, are the most potent effectors of the adaptive immune system and a fundamental component of cancer immunotherapy [20]. The objective of immune-checkpoint inhibitors is to hinder the activity of immune receptors that suppress the immune system and revitalize nonfunctioning T cells, such as CD8+ T cells [21]. Continued exposure of CD8+ T cells to tumor neoantigens can lead to the prolonged presence of immune checkpoint molecules [21, 22]. This state is commonly known as CD8+ T-cell exhaustion and is characterized by a decrease in proliferative capacity, reduced production of effector cytokines, and cytotoxicity [21, 22]. In this state, T cells are unable to attack cancer cells effectively, leading to tumor progression. The population of exhausted PD-1+CD8+ T cells is heterogeneous and can be categorized into subsets based on their PD-1 expression levels, namely PD-1 low and PD-1 high subsets. The PD-1 low subset exhibits a better response to anti-PD-L1 blockade compared to the PD-1 high subset [23]. A recent study in patients with melanoma revealed that the exhausted CD8+ T cell subset with a terminal exhaustion transcriptional signature does not respond well to anti-PD-1/PD-L1 blockade [24]. However, within this subset, those with high levels of the TCF-7 transcription factor, which is associated with a stem-like CD8+ T cell state, showed a better response to anti-PD-1/PD-L1 blockade [24]. In our experiments, we observed that the high-RRM2 group showed increased expression of various immune checkpoint molecules across the three public datasets. These results indicated an increased presence of exhausted CD8+ T cells in the high-RRM2 group. Considering that the high-RRM2 group exhibited a favorable response to anti-PD-1/PD-L1 blockade, this suggests that the high-RRM2 group is likely to have a higher proportion of exhausted CD8+ T cells that respond well to anti-PD-1/PD-L1 blockade.

In patients who did not receive anti-PD-1/PD-L1 blockade, higher expression of RRM2 was associated with a poorer prognosis. However, in patients who received anti-PD-1/PD-L1 blockade, the opposite result was observed. Patients with high expression of RRM2 are expected to have a poorer prognosis due to the

higher expression of immune checkpoints and their immune-suppressed state. However, in cases where patients receive anti-PD-1/PD-L1 blockade treatment, the higher expression of immune checkpoints suggests that they may respond better to anti-PD-1/PD-L1 blockade, leading to an improvement in prognosis.

The high-RRM2 group demonstrated an elevated level of the interferon gamma gene signature in three publicly available LUAD datasets. Interferon gamma plays a crucial role in regulating the PD-L1/PD-1 pathway. The group with a high interferon gamma gene signature showed a favorable response to PD-L1/PD-1 blockade in melanoma, head and neck squamous cell carcinoma and gastric carcinoma [25]. Secretion of interferon gamma by CD8+ lymphocytes upregulates PD-L1 expression in ovarian cancer cells, leading to tumor progression [26]. A positive correlation was observed between interferon-gamma levels and PD-L1 expression in both human and murine glioma [27]. Interferon gamma regulates PD-L1 expression by activating the PD-L1 promoter through the JAK1/JAK2-STAT1/STAT2/STAT3-IRF1 axis in melanoma cell lines [28].

Macrophages play important roles in the immune system and are typically classified into two main phenotypes: pro-inflammatory M1 and anti-inflammatory M2 [29]. M1 macrophages enhance antitumor inflammatory responses by promoting tumor phagocytosis [30]. In contrast, M2 macrophages contribute to tumor progression through immune suppression, angiogenesis, and neovascularization [30]. In certain types of cancers, increased infiltration of M2 macrophages is frequently associated with the development of drug resistance to the PD-1/PD-L1 blockade [31, 32]. Additionally, the response to anti-PD-1 immunotherapy in glioblastoma can be improved by suppressing M2 macrophages via anti-CSF-1R blockade [33]. In the present study, although it was not significant in the CiberSortx results, TIDE analysis showed a significantly lower frequency of M2 macrophages in the high-RRM2 group. Since a low level of M2 macrophages is associated with a favorable response to PD-1/PD-L1 blockade, the low level of M2 macrophages in the high-RRM2 group could potentially impact the responsiveness to PD-1/PD-L1 blockade.

In three public LUAD datasets, the high-RRM2 group exhibited low CAF levels. CAFs, a cell population found within the tumor microenvironment, play a crucial role in promoting tumorigenic characteristics by initiating extracellular matrix remodeling or releasing cytokines [34]. It has been reported that CAFs play a significant role in PD-1/PD-L1 blockade. In advanced NSCLC, previous researchers discovered that CAFs secreted TGF-β1, which utilized the c-Jun N-terminal kinase/activator protein 1 (JNK/AP1) signaling pathway to stimulate the expression of Ln-γ2 in cancer cells [35]. This mechanism results in the formation of a protective barrier that restricts T cell infiltration into the cancerous region. In metastatic urothelial cancer, TGF-β plays a role in shaping the tumor microenvironment by restricting T cell infiltration, consequently suppressing the immune response against tumors [36]. CAFs secrete WNT2, which hinders the differentiation of dendritic cells and consequently diminishes the generation of effector T cells [37].

Xiong et al. showed that RRM2 enhances the expression of PD-L1 in renal cancer cells [12]. RRM2 upregulates PD-L1 expression via the ANXA1/AKT signaling axis [12]. Furthermore, in a renal cell carcinoma mouse model, the co-inhibition of RRM2 and PD-1 resulted in greater suppression of tumor growth than single inhibition alone [12]. Our findings also indicate a positive association between the expression levels of PD-L1 and RRM2 in cell line experiments. We confirmed that RRM2 knockdown in the LUAD cell lines resulted in decreased expression of the PD-L1/ANXA1/AKT pathway. PD-L1 expression is regulated by the PI3K/AKT/mTOR pathway. Inhibitors targeting the PI3K/AKT/mTOR pathway lead to a decrease in PD-L1 expression [38], whereas activation of the AKT/mTOR pathway resulted in the upregulation of PD-L1 expression [39]. ANXA1 activates the PI3K/AKT signaling pathway in cancer cells by interacting with the formyl peptide receptors (FPRs), FPR1 and FPR2 [40, 41]. ANXA1 activates AKT signaling, leading to poor response to trastuzumab-based treatment in breast cancer [41].

The RRM2 inhibitor, 4-hydroxysalicylanilide (HDS), is currently undergoing phase I clinical trials for multiple myeloma (ClinicalTrials.gov: NCT03670173). HDS extended survival in a

xenograft model of multiple myeloma and exhibited synergistic antimyeloma activity when combined with melphalan and bortezomib [42]. In a mouse model of lung squamous cell carcinoma, the novel RRM2 inhibitor, GW8510, has the ability to overcome gemcitabine resistance in cancer cells by inducing autophagy through the downregulation of RRM2 [43]. In a mouse model of triple-negative breast cancer, the ANXA1 inhibitor Boc1 demonstrated the ability decrease tumor size and inhibit Treg cell function [44]. Several targeted inhibitors of PI3K, AKT, and mTOR are currently being developed and investigated in preclinical studies and early phase clinical trials for NSCLC [45]. In a phase 2 clinical trial for breast cancer, the combination of the PD-L1 inhibitor atezolizumab and AKT inhibitor ipatasertib increased the number of Granzyme B+CD8+ T cells [45]. Therefore, the simultaneous inhibition of PD-L1, RRM2, ANXA1, and AKT could be a promising strategy to overcome resistance to PD-1/PD-L1 blockade in LUAD.

Our study has several limitations. First, we validated whether RRM2 expression could predict the response of patients treated with PD-1/PD-L1 blockade therapy. However, the number of patients treated with PD-1/PD-L1 blockade therapy was limited to 63, indicating the need for validation in a larger cohort of patients. Second, we discovered that RRM2 regulated PD-L1 expression through the ANXA1/AKT pathway. However, the primary function of RRM2 is DNA replication and research on its involvement in immunological pathways remains limited. Therefore, extensive functional studies are required to understand the mechanisms by which RRM2 regulates the PD-L1/PD-1 pathway.

We discovered that RRM2 mRNA or protein expression could predict the response to PD-1/PD-L1 blockade therapy in four independent LUAD datasets. RRM2 expression was positively correlated with CD8+ T cell infiltration and the expression of immune checkpoints. Our findings also revealed that the ANXA1/AKT pathway was involved in the regulation of PD-L1 expression by RRM2. In addition to its role as a predictive biomarker, RRM2 may emerge as a novel target for overcoming PD-L1/PD-1 resistance.

## Acknowledgements

This research was supported by the Basic Science Research Program through the National Research Foundation of Korea (NRF) funded by the Ministry of Science, ICT (RS-2023-00249100 for Young Wha Koh).

## Disclosure of conflict of interest

None.

**Address correspondence to:** Dr. Young Wha Koh, Department of Pathology, Ajou University School of Medicine, 206 Worldcup-ro, Yeongtong-gu, Suwon-si, Gyeonggi-do 16499, South Korea. Tel: +82-31-219-7055; Fax: +82-31-219-5934; E-mail: youngwha9556@gmail.com

## References

[1] Garon EB, Rizvi NA, Hui R, Leighl N, Balmanoukian AS, Eder JP, Patnaik A, Aggarwal C, Gubens M, Horn L, Carcereny E, Ahn MJ, Felip E, Lee JS, Hellmann MD, Hamid O, Goldman JW, Soria JC, Dolled-Filhart M, Rutledge RZ, Zhang J, Lunceford JK, Rangwala R, Lubiniecki GM, Roach C, Emancipator K and Gandhi L; KEYNOTE-001 Investigators. Pembrolizumab for the treatment of non-small-cell lung cancer. N Engl J Med 2015; 372: 2018-2028.

[2] Gettinger S, Rizvi NA, Chow LQ, Borghaei H, Brahmer J, Ready N, Gerber DE, Shepherd FA, Antonia S, Goldman JW, Juergens RA, Laurie SA, Nathan FE, Shen Y, Harbison CT and Hellmann MD. Nivolumab monotherapy for first-line treatment of advanced non-small-cell lung cancer. J Clin Oncol 2016; 34: 2980-2987.

[3] Herbst RS, Baas P, Kim DW, Felip E, Perez-Gracia JL, Han JY, Molina J, Kim JH, Arvis CD, Ahn MJ, Majem M, Fidler MJ, de Castro G Jr, Garrido M, Lubiniecki GM, Shentu Y, Im E, Dolled-Filhart M and Garon EB. Pembrolizumab versus docetaxel for previously treated, PD-L1-positive, advanced non-small-cell lung cancer (KEYNOTE-010): a randomised controlled trial. Lancet 2016; 387: 1540-1550.

[4] Mino-Kenudson M. Programmed cell death ligand-1 (PD-L1) expression by immunohistochemistry: could it be predictive and/or prognostic in non-small cell lung cancer? Cancer Biol Med 2016; 13: 157-170.

[5] Kerr KM, Tsao MS, Nicholson AG, Yatabe Y, Wistuba II and Hirsch FR; IASLC Pathology Committee. Programmed death-ligand 1 immunohistochemistry in lung cancer: in what state is this art? J Thorac Oncol 2015; 10: 985-989.

[6] Zhan Y, Jiang L, Jin X, Ying S, Wu Z, Wang L, Yu W, Tong J, Zhang L, Lou Y and Qiu Y. Inhibiting RRM2 to enhance the anticancer activity of chemotherapy. Biomed Pharmacother 2021; 133: 110996.
[7] D'Angiolella V, Donato V, Forrester FM, Jeong YT, Pellacani C, Kudo Y, Saraf A, Florens L, Washburn MP and Pagano M. Cyclin F-mediated degradation of ribonucleotide reductase M2 controls genome integrity and DNA repair. Cell 2012; 149: 1023-1034.
[8] Sun H, Yang B, Zhang H, Song J, Zhang Y, Xing J, Yang Z, Wei C, Xu T, Yu Z, Xu Z, Hou M, Ji M and Zhang Y. RRM2 is a potential prognostic biomarker with functional significance in glioma. Int J Biol Sci 2019; 15: 533-543.
[9] Zhou Z, Song Q, Yang Y, Wang L and Wu Z. Comprehensive landscape of RRM2 with immune infiltration in pan-cancer. Cancers (Basel) 2022; 14: 2938.
[10] Qin Z, Xie B, Qian J, Ma X, Zhang L, Wei J, Wang Z, Fan L, Zhu Z, Qian Z, Yin H, Zhu F and Tan Y. Over-expression of RRM2 predicts adverse prognosis correlated with immune infiltrates: a potential biomarker for hepatocellular carcinoma. Front Oncol 2023; 13: 1144269.
[11] Mao G, Li L, Shan C, Liang B, Ma L and Zhang S. High expression of RRM2 mediated by noncoding RNAs correlates with poor prognosis and tumor immune infiltration of hepatocellular carcinoma. Front Med (Lausanne) 2022; 9: 833301.
[12] Xiong W, Zhang B, Yu H, Zhu L, Yi L and Jin X. RRM2 regulates sensitivity to sunitinib and PD-1 blockade in renal cancer by stabilizing ANXA1 and activating the AKT pathway. Adv Sci (Weinh) 2021; 8: e2100881.
[13] Tang B, Xu W, Wang Y, Zhu J, Wang H, Tu J, Weng Q, Kong C, Yang Y, Qiu R, Zhao Z, Xu M and Ji J. Identification of critical ferroptosis regulators in lung adenocarcinoma that RRM2 facilitates tumor immune infiltration by inhibiting ferroptotic death. Clin Immunol 2021; 232: 108872.
[14] Byeon HE, Haam S, Han JH, Lee HW and Koh YW. Intrinsic and extrinsic transcriptional profiles that affect the clinical response to PD-1 inhibitors in patients with non-small cell lung cancer. Cancers (Basel) 2022; 15: 197.
[15] Cerami E, Gao J, Dogrusoz U, Gross BE, Sumer SO, Aksoy BA, Jacobsen A, Byrne CJ, Heuer ML, Larsson E, Antipin Y, Reva B, Goldberg AP, Sander C and Schultz N. The cBio cancer genomics portal: an open platform for exploring multidimensional cancer genomics data. Cancer Discov 2012; 2: 401-404.
[16] Jiang P, Gu S, Pan D, Fu J, Sahu A, Hu X, Li Z, Traugh N, Bu X, Li B, Liu J, Freeman GJ, Brown MA, Wucherpfennig KW and Liu XS. Signatures of T cell dysfunction and exclusion predict cancer immunotherapy response. Nat Med 2018; 24: 1550-1558.
[17] Newman AM, Steen CB, Liu CL, Gentles AJ, Chaudhuri AA, Scherer F, Khodadoust MS, Esfahani MS, Luca BA, Steiner D, Diehn M and Alizadeh AA. Determining cell type abundance and expression from bulk tissues with digital cytometry. Nat Biotechnol 2019; 37: 773-782.
[18] Munari E, Rossi G, Zamboni G, Lunardi G, Marconi M, Sommaggio M, Netto GJ, Hoque MO, Brunelli M, Martignoni G, Haffner MC, Moretta F, Pegoraro MC, Cavazza A, Samogin G, Furlan V, Mariotti FR, Vacca P, Moretta L and Bogina G. PD-L1 assays 22C3 and SP263 are not interchangeable in non-small cell lung cancer when considering clinically relevant cutoffs: an interclone evaluation by differently trained pathologists. Am J Surg Pathol 2018; 42: 1384-1389.
[19] McCarty KS Jr, Szabo E, Flowers JL, Cox EB, Leight GS, Miller L, Konrath J, Soper JT, Budwit DA, Creasman WT, et al. Use of a monoclonal anti-estrogen receptor antibody in the immunohistochemical evaluation of human tumors. Cancer Res 1986; 46 Suppl: 4244s-4248s.
[20] Farhood B, Najafi M and Mortezaee K. CD8(+) cytotoxic T lymphocytes in cancer immunotherapy: a review. J Cell Physiol 2019; 234: 8509-8521.
[21] Raskov H, Orhan A, Christensen JP and Gögenur I. Cytotoxic CD8+ T cells in cancer and cancer immunotherapy. Br J Cancer 2021; 124: 359-367.
[22] Watowich MB, Gilbert MR and Larion M. T cell exhaustion in malignant gliomas. Trends Cancer 2023; 9: 270-292.
[23] Blackburn SD, Shin H, Freeman GJ and Wherry EJ. Selective expansion of a subset of exhausted CD8 T cells by alphaPD-L1 blockade. Proc Natl Acad Sci U S A 2008; 105: 15016-15021.
[24] Sade-Feldman M, Yizhak K, Bjorgaard SL, Ray JP, de Boer CG, Jenkins RW, Lieb DJ, Chen JH, Frederick DT, Barzily-Rokni M, Freeman SS, Reuben A, Hoover PJ, Villani AC, Ivanova E, Portell A, Lizotte PH, Aref AR, Eliane JP, Hammond MR, Vitzthum H, Blackmon SM, Li B, Gopalakrishnan V, Reddy SM, Cooper ZA, Paweletz CP, Barbie DA, Stemmer-Rachamimov A, Flaherty KT, Wargo JA, Boland GM, Sullivan RJ, Getz G and Hacohen N. Defining T cell states associated with response to checkpoint immunotherapy in melanoma. Cell 2018; 175: 998-1013, e20.
[25] Ayers M, Lunceford J, Nebozhyn M, Murphy E, Loboda A, Kaufman DR, Albright A, Cheng JD, Kang SP, Shankaran V, Piha-Paul SA, Yearley J,

Seiwert TY, Ribas A and McClanahan TK. IFN-γ-related mRNA profile predicts clinical response to PD-1 blockade. J Clin Invest 2017; 127: 2930-2940.

[26] Abiko K, Matsumura N, Hamanishi J, Horikawa N, Murakami R, Yamaguchi K, Yoshioka Y, Baba T, Konishi I and Mandai M. IFN-γ from lymphocytes induces PD-L1 expression and promotes progression of ovarian cancer. Br J Cancer 2015; 112: 1501-1509.

[27] Qian J, Wang C, Wang B, Yang J, Wang Y, Luo F, Xu J, Zhao C, Liu R and Chu Y. The IFN-γ/PD-L1 axis between T cells and tumor microenvironment: hints for glioma anti-PD-1/PD-L1 therapy. J Neuroinflammation 2018; 15: 290.

[28] Garcia-Diaz A, Shin DS, Moreno BH, Saco J, Escuin-Ordinas H, Rodriguez GA, Zaretsky JM, Sun L, Hugo W, Wang X, Parisi G, Saus CP, Torrejon DY, Graeber TG, Comin-Anduix B, Hu-Lieskovan S, Damoiseaux R, Lo RS and Ribas A. Interferon receptor signaling pathways regulating PD-L1 and PD-L2 expression. Cell Rep 2017; 19: 1189-1201.

[29] Wynn TA and Vannella KM. Macrophages in tissue repair, regeneration, and fibrosis. Immunity 2016; 44: 450-462.

[30] Liu J, Geng X, Hou J and Wu G. New insights into M1/M2 macrophages: key modulators in cancer progression. Cancer Cell Int 2021; 21: 389.

[31] Zhu Z, Zhang H, Chen B, Liu X, Zhang S, Zong Z and Gao M. PD-L1-mediated immunosuppression in glioblastoma is associated with the infiltration and M2-polarization of tumor-associated macrophages. Front Immunol 2020; 11: 588552.

[32] Kim YJ, Won CH, Lee MW, Choi JH, Chang SE and Lee WJ. Correlation between tumor-associated macrophage and immune checkpoint molecule expression and its prognostic significance in cutaneous melanoma. J Clin Med 2020; 9: 2500.

[33] Cui X, Ma C, Vasudevaraja V, Serrano J, Tong J, Peng Y, Delorenzo M, Shen G, Frenster J, Morales RT, Qian W, Tsirigos A, Chi AS, Jain R, Kurz SC, Sulman EP, Placantonakis DG, Snuderl M and Chen W. Dissecting the immunosuppressive tumor microenvironments in glioblastoma-on-a-Chip for optimized PD-1 immunotherapy. Elife 2020; 9: e52253.

[34] Kalluri R. The biology and function of fibroblasts in cancer. Nat Rev Cancer 2016; 16: 582-598.

[35] Li L, Wei JR, Dong J, Lin QG, Tang H, Jia YX, Tan W, Chen QY, Zeng TT, Xing S, Qin YR, Zhu YH, Li Y and Guan XY. Laminin γ2-mediating T cell exclusion attenuates response to anti-PD-1 therapy. Sci Adv 2021; 7: eabc8346.

[36] Mariathasan S, Turley SJ, Nickles D, Castiglioni A, Yuen K, Wang Y, Kadel EE III, Koeppen H, Astarita JL, Cubas R, Jhunjhunwala S, Banchereau R, Yang Y, Guan Y, Chalouni C, Ziai J, Şenbabaoğlu Y, Santoro S, Sheinson D, Hung J, Giltnane JM, Pierce AA, Mesh K, Lianoglou S, Riegler J, Carano RAD, Eriksson P, Höglund M, Somarriba L, Halligan DL, van der Heijden MS, Loriot Y, Rosenberg JE, Fong L, Mellman I, Chen DS, Green M, Derleth C, Fine GD, Hegde PS, Bourgon R and Powles T. TGFβ attenuates tumour response to PD-L1 blockade by contributing to exclusion of T cells. Nature 2018; 554: 544-548.

[37] Huang TX, Tan XY, Huang HS, Li YT, Liu BL, Liu KS, Chen X, Chen Z, Guan XY, Zou C and Fu L. Targeting cancer-associated fibroblast-secreted WNT2 restores dendritic cell-mediated antitumour immunity. Gut 2022; 71: 333-344.

[38] Sun SY. Searching for the real function of mTOR signaling in the regulation of PD-L1 expression. Transl Oncol 2020; 13: 100847.

[39] Lastwika KJ, Wilson W 3rd, Li QK, Norris J, Xu H, Ghazarian SR, Kitagawa H, Kawabata S, Taube JM, Yao S, Liu LN, Gills JJ and Dennis PA. Control of PD-L1 expression by oncogenic activation of the AKT-mTOR pathway in non-small cell lung cancer. Cancer Res 2016; 76: 227-238.

[40] Khau T, Langenbach SY, Schuliga M, Harris T, Johnstone CN, Anderson RL and Stewart AG. Annexin-1 signals mitogen-stimulated breast tumor cell proliferation by activation of the formyl peptide receptors (FPRs) 1 and 2. FASEB J 2011; 25: 483-496.

[41] Berns K, Sonnenblick A, Gennissen A, Brohée S, Hijmans EM, Evers B, Fumagalli D, Desmedt C, Loibl S, Denkert C, Neven P, Guo W, Zhang F, Knijnenburg TA, Bosse T, van der Heijden MS, Hindriksen S, Nijkamp W, Wessels LF, Joensuu H, Mills GB, Beijersbergen RL, Sotiriou C and Bernards R. Loss of ARID1A activates ANXA1, which serves as a predictive biomarker for trastuzumab resistance. Clin Cancer Res 2016; 22: 5238-5248.

[42] Xie Y, Wang Y, Xu Z, Lu Y, Song D, Gao L, Yu D, Li B, Chen G, Zhang H, Feng Q, Zhang Y, Hu K, Huang C, Peng Y, Wu X, Mao Z, Shao J, Zhu W and Shi J. Preclinical validation and phase I trial of 4-hydroxysalicylanilide, targeting ribonucleotide reductase mediated dNTP synthesis in multiple myeloma. J Biomed Sci 2022; 29: 32.

[43] Chen P, Wu JN, Shu Y, Jiang HG, Zhao XH, Qian H, Chen K, Lan T, Chen CG and Li J. Gemcitabine resistance mediated by ribonucleotide reductase M2 in lung squamous cell carcinoma is reversed by GW8510 through au-

tophagy induction. Clin Sci (Lond) 2018; 132: 1417-1433.
[44] Bai F, Zhang P, Fu Y, Chen H, Zhang M, Huang Q, Li D, Li B and Wu K. Targeting ANXA1 abrogates Treg-mediated immune suppression in triple-negative breast cancer. J Immunother Cancer 2020; 8: e000169.
[45] Tan AC. Targeting the PI3K/Akt/mTOR pathway in non-small cell lung cancer (NSCLC). Thorac Cancer 2020; 11: 511-518.

**Supplementary Table 1.** Univariate and multivariate analyses of overall survival for PanCancer Atlas cohort without PD-L1/PD-1 treatment

| Covariate | Univariate | | | Multivariate | | |
|---|---|---|---|---|---|---|
| | HR | 95% CI | *P*-value† | HR | 95% CI | *P*-value† |
| Age (≥65 y vs. <65 y) | 1.015 | 0.756-1.363 | 0.920 | | | |
| Sex (male vs. female) | 0.947 | 0.707-1.268 | 0.714 | | | |
| Stage (III-IV vs. I-II) | 2.687 | 1.972-3.663 | <0.001 | 2.519 | 1.841-3.445 | <0.001 |
| RRM2 (high vs. low) | 1.650 | 1.224-2.226 | 0.001 | 1.476 | 1.090-1.999 | 0.012 |

Abbreviations: CI, confidence interval; HR, hazard ratio. †The Cox proportional-hazard test.

**Supplementary Table 2.** Univariate and multivariate analyses of overall survival for Oncosg cohort without PD-L1/PD-1 treatment

| Covariate | Univariate | | | Multivariate | | |
|---|---|---|---|---|---|---|
| | HR | 95% CI | *P*-value† | HR | 95% CI | *P*-value† |
| Age (≥65 y vs. <65 y) | 1.544 | 0.837-2.850 | 0.165 | | | |
| Sex (male vs. female) | 1.786 | 0.969-3.291 | 0.063 | | | |
| Stage (III-IV vs. I-II) | 2.768 | 1.480-5.177 | 0.001 | 2.538 | 1.352-4.764 | 0.004 |
| Smoking history (+ vs. -) | 1.730 | 0.940-3.184 | 0.078 | | | |
| RRM2 (high vs. low) | 2.092 | 1.110-3.943 | 0.023 | 1.865 | 0.982-4.764 | 0.057 |

Abbreviations: CI, confidence interval; HR, hazard ratio. †The Cox proportional-hazard test.

**Supplementary Table 3.** Univariate and multivariate analyses of overall survival for IHC cohort without PD-L1/PD-1 treatment

| Covariate | Univariate | | | Multivariate | | |
|---|---|---|---|---|---|---|
| | HR | 95% CI | *P*-value† | HR | 95% CI | *P*-value† |
| Age (≥65 y vs. <65 y) | 1.122 | 0.740-1.700 | 0.588 | | | |
| Sex (male vs. female) | 1.865 | 1.183-2.941 | 0.007 | 1.902 | 0.946-3.826 | 0.071 |
| Stage (III-IV vs. I-II) | 2.952 | 1.944-4.484 | <0.001 | 2.082 | 1.310-3.310 | 0.002 |
| Smoking history (+ vs. -) | 1.580 | 1.004-2.486 | 0.048 | 0.755 | 0.383-1.491 | 0.419 |
| RRM2 (high vs. low) | 6.493 | 3.911-10.77 | <0.001 | 6.353 | 3.635-11.10 | <0.001 |

Abbreviations: CI, confidence interval; HR, hazard ratio. †The Cox proportional-hazard test.

**Supplementary Table 4.** Univariate and multivariate analyses of progression-free survival for mRNA cohort with PD-L1/PD-1 treatment

| Covariate | Univariate | | | Multivariate | | |
|---|---|---|---|---|---|---|
| | HR | 95% CI | *P*-value† | HR | 95% CI | *P*-value† |
| Age (≥65 y vs. <65 y) | 0.907 | 0.396-2.077 | 0.817 | | | |
| Sex (male vs. female) | 0.526 | 0.218-1.270 | 0.153 | 0.446 | 0.181-1.099 | 0.079 |
| Stage (IV vs. III) | 1.990 | 0.464-8.541 | 0.354 | | | |
| Smoking history (+ vs. -) | 1.108 | 0.294-4.178 | 0.879 | | | |
| RRM2 (high vs. low) | 0.259 | 0.076-0.882 | 0.031 | 0.234 | 0.068-0.804 | 0.021 |

Abbreviations: CI, confidence interval; HR, hazard ratio. †The Cox proportional-hazard test.

**Supplementary Table 5.** Univariate and multivariate analyses of progression-free survival for IHC cohort with PD-L1/PD-1 treatment

| Covariate | Univariate | | | Multivariate | | |
|---|---|---|---|---|---|---|
| | HR | 95% CI | *P*-value† | HR | 95% CI | *P*-value† |
| Age (≥65 y vs. <65 y) | 0.978 | 0.945-1.012 | 0.196 | | | |
| Sex (male vs. female) | 0.429 | 0.210-0.876 | 0.020 | 0.095 | 0.256-1.114 | 0.095 |
| Stage (IV vs. III) | 1.065 | 0.412-2.753 | 0.896 | | | |
| Smoking history (+ vs. -) | 1.458 | 0.540-3.938 | 0.457 | | | |
| RRM2 (high vs. low) | 0.360 | 0.140-0.928 | 0.034 | 0.089 | 0.160-1.137 | 0.089 |

Abbreviations: CI, confidence interval; HR, hazard ratio. †The Cox proportional-hazard test.